Research Article

Yijie Li, Muhammad Imran Anwar, Nek Muhammad Katbar, M. Prakash, Muhammad Saqlain, Muhammad Waqas, Abdul Wahab, Wasim Jamshed*, Mohamed R. Eid, and Ahmed M. Hassan

Analysis of magnetized micropolar fluid subjected to generalized heat-mass transfer theories

https://doi.org/10.1515/phys-2023-0117
received September 10, 2022; accepted September 21, 2023

Abstract: In this study, the steady 2D flow of micropolar fluid *via* a vertical surface is taken into account. The magnetohydrodynamics applied normally to the flow direction at a vertical surface in the presence of temperature-dependent attributes. The effect of the chemical reaction under the generalized Fourier–Fick law is considered to investigate the heat transference rate at the vertical sheet. Under the flow assumptions, the boundary layer approximations were applied to the nonlinear differential equations and partial differential equations were obtained. The use of similarity modifications allows for a reduction in the number of partial differential equations. The resulting ordinary differential equations are then resolved numerically using a technique known as the homotopy analysis method. The results reveal that microparticle suspensions have a significant impact on the flowing domain when varied fluid characteristics are utilized. The effect of potential factors on flow, micro-rotation velocities, temperature, drag force factor, and heat transport rate is investigated. The obtained results show that the velocity profile and micropolar function increase for larger values of micropolar parameters. Drag force effects are also seen, and required outcomes are observed to be in outstanding accord with the available literature. Significant results of this work were toward the velocity function, which gets reduced with increasing magnetic field parameter values, but the velocity function enhances for higher values of β and λ. On temperature distribution, it decreased for higher values of ϵ_1 and temperature profile declines due to higher values of Pr, γ_2 and γ_1 or both cases of $\delta > 0$ and $\delta < 0$. The higher values of Sc resist declining the temperature function at the surface.

Keywords: generalized Fourier–Fick laws, micropolar fluid, mixed convection, heat generation, temperature dependent properties

*** Corresponding author: Wasim Jamshed**, Department of Mathematics, Capital University of Science and Technology (CUST), Islamabad, 44000, Pakistan, e-mail: wasiktk@hotmail.com
Yijie Li: School of Computer Science, University of St Andrews, St Andrews KY16 9SX, United Kingdom
Muhammad Imran Anwar: Department of Mathematics, University of Sargodha, Sargodha, Pakistan; Higher Education Department, Lahore, Pakistan; Department of Mathematics, School of Sciences and Humanities, Nazarbayev University, Astana, Kazakhstan
Nek Muhammad Katbar: School of Mathematics and Statistics, Central South University, Changsha, 410083, China; Mehran UET Shaheed Zulfiqar Ali Bhutto Campus Khairpur, Khairpur, Pakistan
M. Prakash: Department of Mathematics, KPR Institute of Engineering and Technology, Coimbatore, Tamil Nadu, 641407, India
Muhammad Saqlain: Department of Mathematics, University of Sargodha, Sargodha, Pakistan
Muhammad Waqas: NUTECH School of Applied Sciences and Humanities, National University of Technology, Islamabad, Pakistan; Department of Mechanical Engineering, Lebanese American University, Beirut, Lebanon
Abdul Wahab: Department of Mathematics, School of Sciences and Humanities, Nazarbayev University, Astana, Kazakhstan
Mohamed R. Eid: Department of Mathematics, Faculty of Science, New Valley University, Al-Kharga, Al-Wadi Al-Gadid, 72511 Egypt; Finance and Insurance Department, College of Business Administration, Northern Border University, Arar, 1321, Saudi Arabia
Ahmed M. Hassan: Center of Research, Faculty of Engineering, Future University in Egypt New Cairo, New Cairo, 11835, Egypt

Nomenclature

(u, v)	horizontal and vertical fluid velocities
ρ	fluid density
ν	kinematic viscosity
k	vertex viscosity
g	gravitational acceleration
β_1	thermal expansion coefficient
β_2	solutal expansion coefficient
γ^*	spin gradient viscosity
j	density due to micro-inertia
λ_T	thermal relaxation time flux
λ_C	solutal relaxation time flux

c_p	specific heat
Q	heat generation coefficient
m_0	boundary layer parameter
N	velocity due to micro-rotation
T_w	wall temperature
C_w	wall concentration
δ	heat generation/absorption parameter

1 Introduction

Fourier's relation [1] has been used in various industrial and technological applications for energy transportation by means of heat conduction. While implementing this relation, a parabolic type of energy expression is observed; this is the inadequacy of this relation. Different researchers try to overcome this inadequacy in Fourier's relation. Cattaneo [2] introduced the thermal relaxation parameter in Fourier's relation. Cattaneo analysis [2] has been improved significantly by Christov [3] with the addition of Oldroyd's type upper convective derivative in the thermal relaxation term. In micropolar liquids, every molecule having a limited size contains a microstructure that can turn and twist freely regardless of the movement of the centroid of the molecule. The micropolar hypothesis provides an elective way to deal with mathematically settling the micro-scale liquid elements. Nonlinear convective stagnation point flow under modified Fourier's and Fick laws subject to temperature-dependent thermal conductivity is elaborated by Zubair *et al.* [4]. Waqas *et al.* [5] investigated revised Burgers' liquid by using enhanced Fourier–Fick laws in stretchable flow under the impermeable stretching sheet. Novel nonlinear models related to micropolar fluid regarding boundary layer flow are established by Sui *et al.* [6]. Mixed convective Burger's fluid flow on a stretching surface considering heat generation and variant thermal conductance is elaborated by Waqas *et al.* [7]. Anwar *et al.* [8] discussed homotopic solutions for Jaffrey fluid exposure based on modified Fourier's and Fick's principles. Bioconvection magnetohydrodynamics (MHD) Carreau nanoliquid flowing over a parabolic sheet considering improved Fourier's and Fick rules is presented by Khan *et al.* [9]. Three-dimensional Sisko liquid considering global heat flux and mass diffusion relationships along with temperature-based thermal conductance is numerically investigated by Khan *et al.* [10]. Hayat *et al.* [11] used Fourier–Fick laws along with variable thermal conductivity to study the Jaffrey fluid flowing by a rotary disk having a changeable thickness. Devi and Prakash [12] explored the effects of temperature-dependent characteristics of liquid on hydro-magnetic flowing over a slandering stretching sheet. The Fourier relation is ineffective for solving situations that include a large thermal gradient, temperatures below absolute zero, short temperature shifts, and nano/micro-scales in space and time [13]. Nanoliquid squeezed flow subjected to generalized fluxes is presented by Noor *et al.* [14]. The traditional heat conduction relation [15] communicates heat flux precisely to temperature gradient utilizing the coefficient of thermal conductivity. For illustration, Daneshjou *et al.* [16] formulated time-dependent flow in 2D orthotropic non-Fourier based hollow cylinders. Khan *et al.* [17] reported research that examined the influence of thermal radiation on the flow of chemically reacted Burger's liquid toward a heated surface. By applying the coefficient of thermal conductivity, the conventional relation for heat conduction [18] can accurately convey the relationship between heat flow and temperature variation. For the purpose of illustrative purposes, Alsaedi *et al.* [19] developed chemically reacted flow in the stagnation area of Burgers liquid. Tibullo and Zampoli [20] recognized individuality outcomes for incompressible nature problems subjected to modified Fourier law. Analytical consideration of forced convection stratified Burger's fluid movement was given by Waqas *et al.* [21] in accordance with the improved Fourier law. Khan *et al.* [22] studied the effects of using an enhanced version of the Fourier law on changeable liquid characteristics in a stratified Carreau nanoliquid. The thermally radiating stratified Jeffrey nanoliquid that was exposed to buoyancy forces was proposed by Waqas *et al.* [23]. Heat conduction expression *via* the Fourier situation has a parabolic form, which enables thermal instabilities to communicate the thermal propagation of waves having infinite velocity. This phenomenon has to be enhanced at very smaller time scales and lengths in only a few nano/micro-scale structures. A large number of scholars have made contributions to additional advances that have been analyzed using the Cattaneo model.

The study of the behavior of non-Newtonian liquids has recently gained attention due to its rheological applications in chemically and mechanistic manufacturing activities. Among the industrial uses are oil extraction, artificial production development, nutrition administration, and the performing of coats and oils. Non-Newtonian liquids are commonly used in production and manufacturing processes. There is a non-linear relationship among shearing stress and shearing rate, and the shearing rate is modified by the shear stress period. In the literature, several rheological models exist to illustrate certain physical features of non-Newtonian liquids, such as the viscoelastic fluid model and secondly ordered liquid type, Walter's liquid type, Cattaneo/Christov heat fluxing type, Maxwell liquid framework, and so on. Furthermore, the micro-polarized liquid type is an important model for non-Newtonian liquids for understanding the provenances of liquid transmission and heat transference in several complex liquid-flowing situations.

The traditional Navier–Stokes principal hydrodynamic concept has important shortcomings, such as the inability to depict liquids with the rotational, body downforce, couple-stress, microstructures, and micro rotations, which are critical in analyzing the flowing behavior of liquids such as melted crystalline, polymer liquids, hemoglobin, colloids' liquids, lifeblood serum, actual liquids with postponements, dye, and so on. The liquid rapidity is sufficient to define the flowing issue of a liquid containing suspensions of stiff molecules or micro-structural these fluids, but the angular impetus is also necessary since each particle in the liquid rotates separately along an axis of movement. Eringen [24] developed the micro-polarity liquid concept to quantify the impacts of micro inertia and micro rotation that the traditional hydrodynamic framework does not comprehend, considering this empathic behavior of the fluid molecules into consideration. Khedr *et al.* [25] studied micro-polar liquid flowing across an expanded plate with heat generating (absorbing). Ishak [26] and Hussain *et al.* [27] studied the effect of radiative fluxing on the temperature boundary layer movement of a micro polarity liquid over a stretchable plate. An examination [28] used an exponential declining porousness sheet to investigate micropolar fluid and heat-flowing transfer. The results of Ohmic heating and viscidness dissipative of micro polarity liquid flow *via* an expanded plate were presented by Haque *et al.* [29]. Numerous studies have extensively examined the micro-polar liquid in different spatial formations, as seen by the publications [30–32].

Nevertheless, boundary layer issues with various thicknesses are commonly encountered in engineering disciplines. The researchers became interested in analyzing the flow, heat flux, and diffusion attributes *via* a stretchable plate with a changeable thickener due to its outstanding significance in manufacturing and production developments such as mechanical systems, architectural styles, maritime and aerospace structural systems, powder metallurgy, polymer extruding, and metallurgic progressions. Fang *et al.* [33] quantitatively investigated the varied thicknesses' impact on boundary layer movement through the stretchable plate, displaying the shift in rapidity and shearing stress of a plate affected by its non-uniformity. Khader and Megahed [34] used a similar geometry to investigate the impact of slippage rapidity and exponential rapidity on the movement of a Newtonian fluid. Using the same configuration, Hayat *et al.* [35] studied the magneto flowing of a heat fluxing of Cattaneo/Christov kind for non-Newtonian liquids. Cortell [36], on the other hand, addressed heat transmission through a viscidness flowing. Yang *et al.* [37] investigated the rapidity and temperature of a varying extended plate in the presence of double fractions of Maxwell fluid. Abdel-wahed *et al.* [38] investigated heat transmission and the transmission of a nanoliquid over a moving surface with changing thicknesses. Few studies on different aspects of physical phenomena were analyzed by various researchers [39–47]. Because it is used in ablation cooling, rocket motor burning, pulmonary circuit air movement, and binary gas dispersion, fluidization in tubes is prevalent in industrial and molecular genetics. Fluid properties such as diffusion coefficient, viscosity, conductance, and so on are assumed to remain unchanged for the dexterity of analysis. However, diverse fluid qualities are used in food processing, fiber and wire coating, extrusion processes, chemical manufacturing aids, and other activities. The frictional force caused by viscosity determines the amount of heat transferred by the flowing and is critical in the compilation of fluid measuring for flowing visualization. When the viscous dissipative flow in nearly all actual fluids is observed, the viscidity changes with temperature influences. The viscidity of several fluids, such as honey, syrup, and blood, is affected by temperature. Thermal conductance is an important thermophysical property that impacts the rate of heat transfer in micropolar fluids, which is important when working with heat-generation items like electrical equipment and heat-resistant composites.

With the insight of the aforementioned kind of literature, this work was planned to study the significant thermal characteristic aspects of micro-polar fluid in a chemical reactive environment. Toward the applicability in energy industries, the heat transference analysis has been made in the presence of varying qualities of thermal conductivity and mass diffusivity under generalized Fourier–Fick laws. The novelty of this work can be noted that to the best of the authors' view, this work could be a fresh attempt to study the effects of MHD-based micropolar fluid flow with temperature-dependent properties on a vertical stretching sheet. It will be interesting to explore how under this above circumstance how the MHD-based micro polar fluid flow behaves while passing over another shape with various physical constraints.

2 Mathematical modelling

We formulated the incompressible steady 2D flow of micropolar fluid under generalized Fourier–Fick laws. Heat generation aspects are included. Also, variable thermal conductivity and mass diffusivity are introduced. Non-Newtonian mixed convective flow is considered. The expressions governing the micropolar fluid flow are

$$\nabla \cdot \mathbf{V} = \mathbf{0}, \tag{1}$$

$$\rho \frac{\mathrm{D}\mathbf{V}}{\mathrm{D}t} = -\nabla p + (\mu + k)\nabla^2 \mathbf{V} + k\nabla \times \mathbf{N}, \tag{2}$$

$$\rho j\frac{\mathrm{D}\mathbf{N}}{\mathrm{D}t} = \gamma\nabla(\nabla\cdot\mathbf{N}) - \gamma\nabla\times(\nabla\times\mathbf{N}) + k\nabla\times\mathbf{V} - 2k\mathbf{N}, \tag{3}$$

where $\frac{\mathrm{D}}{\mathrm{D}t}$ represents the material derivative, $(\mathbf{V},\mathbf{N})$ represents the (velocity, microrotation) vectors, j and ρ illustrate the fluid gyration factor and density, μ represents the dynamic viscosity, and (k,γ) represents the (vortex, spin gradient) viscosity.

The governing boundary-layer equations under the aforesaid assumptions are as follows [26]:

$$\frac{\partial u}{\partial x} + \frac{\partial v}{\partial y} = 0, \tag{4}$$

$$u\frac{\partial u}{\partial x} + v\frac{\partial u}{\partial y} = \left(\nu + \frac{k}{\rho}\right)\left(\frac{\partial^2 u}{\partial y^2}\right) + \left(\frac{k}{\rho}\right)\frac{\partial N}{\partial y} + g[\beta_1(T - T_\infty) + \beta_2(C - C_\infty)] - \frac{\sigma {B_0}^2 u}{\rho}, \tag{5}$$

$$u\frac{\partial N}{\partial x} + v\frac{\partial N}{\partial y} = \frac{\gamma^*}{\rho j}\frac{\partial^2 N}{\partial y^2} - \frac{k}{\rho j}\left(\frac{\partial u}{\partial y} + 2N\right), \tag{6}$$

$$u\frac{\partial T}{\partial x} + v\frac{\partial T}{\partial y} + \lambda_\mathrm{T}\begin{pmatrix} u\frac{\partial u}{\partial x}\frac{\partial T}{\partial x} + v\frac{\partial v}{\partial y}\frac{\partial T}{\partial y} + v\frac{\partial u}{\partial y}\frac{\partial T}{\partial x} \\ + 2uv\frac{\partial^2 T}{\partial x\partial y} + u^2\frac{\partial^2 T}{\partial x^2} \\ + v^2\frac{\partial^2 T}{\partial y^2} - \frac{Q}{\rho c_\mathrm{p}}\left(u\frac{\partial T}{\partial x} + v\frac{\partial T}{\partial y}\right) \end{pmatrix} = \frac{1}{\rho c_\mathrm{p}}\frac{\partial}{\partial y}\left(K(T)\frac{\partial T}{\partial y}\right) + \frac{Q}{\rho c_\mathrm{p}}(T - T_\infty), \tag{7}$$

$$u\frac{\partial C}{\partial x} + v\frac{\partial C}{\partial y} + \lambda_\mathrm{C}\begin{pmatrix} u\frac{\partial u}{\partial x}\frac{\partial C}{\partial x} + v\frac{\partial v}{\partial y}\frac{\partial C}{\partial y} + v\frac{\partial u}{\partial y}\frac{\partial C}{\partial x} \\ + 2uv\frac{\partial^2 C}{\partial x\partial y} + u^2\frac{\partial^2 C}{\partial x^2} + v^2\frac{\partial^2 C}{\partial y^2} \end{pmatrix} = \frac{\partial}{\partial y}\left(D(C)\frac{\partial C}{\partial y}\right). \tag{8}$$

Boundary constraints used for this inspection are [26]

$$\left.\begin{aligned} u = U_\mathrm{w}(x) = cx,\ N = -m_0\frac{\partial u}{\partial y}, v = 0, \\ T = T_\mathrm{w},\ C = C_\mathrm{w}\ \text{at}\ y = 0, \\ u\to 0,\ T\to T_\infty,\ N\to 0,\ \ C\to C_\infty\ \text{when}\ y\to\infty, \end{aligned}\right\} \tag{9}$$

where (u,v) represents the horizontal and vertical fluid velocities, ρ represents the fluid density, ν represents the kinematic viscosity, k represents the vertex viscosity, g represents the gravitational acceleration, β_1 represents the thermal expansion coefficient, β_2 represents the solutal expansion coefficient, γ^* is the spin gradient viscosity, j signifies the density due to micro-inertia, λ_T is the thermal relaxation time flux, λ_C is the solutal relaxation time flux, c_p is the specific heat, and Q is the heat generation coefficient.

Regarding the boundary conditions, c is the constant, m_0 is the boundary layer parameter, N velocity due to micro-rotation, T, T_w and C, C_w represent the fluid, wall temperature, and concentricity of the normal regime, and T_∞ and C_∞ denote the fluid temperature and concentricity of ambient regime correspondingly.

Mathematically variable thermal conductivity and mass diffusivity are defined as follows:

$$K(T) = K_\infty(\epsilon_1\theta(\eta) + 1),$$
$$D(C) = D_\infty(\epsilon_2\phi(\eta) + 1),$$

where K_∞ and D_∞ are ambient fluid thermal conductivity and mass diffusivity, and ε_1 and ε_2 are arbitrary small parameters. By applying a flowing group of transformations

$$\left.\begin{aligned} \eta = y\sqrt{\frac{c}{\nu}},\ N = cx\left(\sqrt{\frac{c}{\nu}}\right)g(\eta),\ u = cxf'(\eta), \\ v = -\sqrt{c\nu}f(\eta), \\ \theta(\eta)(T_\mathrm{w} - T_\infty) = T - T_\infty,\ \phi(\eta)(C_\mathrm{w} - C_\infty) = C - C_\infty, \end{aligned}\right\} \tag{10}$$

Eq. (4) is derived obviously while formulas (5)–(8) are as follows:

$$(1 + K)f''' + ff'' - f'^2 + g'K + \lambda(\theta + \beta\phi)\theta - M^2 f' = 0, \tag{11}$$

$$\left(1 + \frac{K}{2}\right)g'' + g'f - gf' - K(f'' + 2g) = 0, \tag{12}$$

$$(1 + \epsilon_1\theta)\theta'' + \epsilon_1\theta'^2 + \mathrm{Pr}f\theta' + \mathrm{Pr}\delta\theta - \mathrm{Pr}\delta\gamma_1 f\theta' - \mathrm{Pr}\gamma_1(ff'\theta' + f^2\theta'') = 0, \tag{13}$$

$$(1 + \epsilon_2\phi)\phi'' + \epsilon_2\phi'^2 + \mathrm{Sc}f\phi' - \mathrm{Sc}\gamma_2(ff'\phi' + f^2\phi'') = 0, \tag{14}$$

$$f'(0) = 1, f(0) = 0,\ f'(\infty)\to 0, \tag{15}$$

$$g(0) = -m_0 f''(0),\ g(\infty)\to 0, \tag{16}$$

$$\theta(0) = 1,\ \theta(\infty)\to 0, \tag{17}$$

$$\phi(0) = 1,\ \phi(\infty)\to 0. \tag{18}$$

The skin frictional factor in dimensionless structure is

$$C_{f_x}\mathrm{Re}_x^{1/2} = (1 + (1 - m_0)K)f''(0). \tag{19}$$

3 Solution procedure

The homotopy analysis method (HAM) [48] is utilized to calculate the convergent outcomes of non-dimensional expressions (11)–(14) while considering the imposed boundary conditions (15)–(18). The initial guesses ($f_0(\eta)$, $g_0(\eta)$, $\theta_0(\eta)$, $\phi_0(\eta)$),

as well as the necessary auxiliary operators ($L_f,\ L_g,\ L_\theta,\ L_\phi$) for HAM computations, are as follows:

$$f_0(\eta) = 1 - e^{-\eta},\ g_0(\eta) = m_0 e^{-\eta},\ \theta_0(\eta) = \exp(-\eta),\ \phi_0(\eta) = \exp(-\eta), \tag{20}$$

$$L_f = f''' - f',\ L_g = g'' - g',\ L_\theta = \theta'' - \theta,\ L_\phi = \phi'' - \phi. \tag{21}$$

The operators ($L_f,\ L_g,\ L_\theta,\ L_\phi$) must validate the ensuing properties:

$$L_f(B_1^* + B_2^* e^{\eta} + B_3^* e^{-\eta}) = 0,\ L_g(B_4^* e^{\eta} + B_5^* e^{-\eta}) = 0, L_\theta(B_6^* e^{\eta} + B_7^* e^{-\eta}) = 0,\ L_\phi(B_8^* e^{\eta} + B_9^* e^{-\eta}) = 0, \tag{22}$$

where B_i^* ($i = 1-9$) signify arbitrary factors.

Now describing the expressions (15)–(18) at the zeroth order, one has

$$(1 - w^*)L_f[\hat{f}(\eta;w^*) - f_0(\eta)] = w^*\hbar_f N_f[\hat{f}(\eta;w^*), \hat{\theta}(\eta;w^*), \hat{\phi}(\eta;w^*)], \tag{23}$$

$$(1 - w^*)L_g[\hat{g}(\eta;w^*) - g_0(\eta)] = w^*\hbar_g N_g[\hat{f}(\eta;w^*), \hat{g}(\eta;w^*)], \tag{24}$$

$$(1 - w^*)L_\theta[\hat{\theta}(\eta;w^*) - \theta_0(\eta)] = w^*\hbar_\theta N_\theta[\hat{f}(\eta;w^*), \hat{\theta}(\eta;w^*)], \tag{25}$$

$$(1 - w^*)L_\phi[\hat{\phi}(\eta;w^*) - \phi_0(\eta)] = w^*\hbar_\phi N_\phi[\hat{f}(\eta;w^*), \hat{\phi}(\eta;w^*)], \tag{26}$$

$$\begin{aligned}\hat{f}(0;w^*) = 0,\ \hat{f}'(0;w^*) = 1,\ \hat{f}'(\infty;w^*) = 0,\ \hat{g}(0;w^*) = -m_0\hat{f}''(0;w^*),\ \hat{g}(\infty;w^*)\\ = 0, \hat{\theta}(0;w^*) = 1,\ \hat{\theta}(\infty;w^*) = 0,\ \hat{\phi}(0;w^*) = 1,\ \hat{\phi}(\infty;w^*) = 0,\end{aligned} \tag{27}$$

$$\begin{aligned}N_f[\hat{f}(\eta;w^*), \hat{\theta}(\eta, w^*), \hat{\phi}(\eta;w^*)] = (1 + K)\frac{\partial^3\hat{f}(\eta;w^*)}{\partial\eta^3} + (\hat{f}(\eta, w^*)\frac{\partial^2\hat{f}(\eta;w^*)}{\partial\eta^2} - \left(\frac{\partial\hat{f}(\eta;w^*)}{\partial\eta}\right)^2 + K\frac{\partial\hat{g}(\eta;w^*)}{\partial\eta}\\ - M^2\frac{\partial\hat{f}(\eta;w^*)}{\partial\eta} + \lambda(\hat{\theta}(\eta;w^*) + \beta\hat{\phi}(\eta;w^*))\hat{\theta}(\eta;w^*),\end{aligned} \tag{28}$$

$$N_g[\hat{f}(\eta;w^*), \hat{g}(\eta;w^*)] = \left(1 + \frac{K}{2}\right)\frac{\partial^2\hat{g}(\eta;w^*)}{\partial\eta^2} + \hat{f}(\eta;w^*)\frac{\partial\hat{g}(\eta;w^*)}{\partial\eta} - \frac{\partial\hat{f}(\eta;w^*)}{\partial\eta}\hat{g}(\eta;w^*) - K\left(2\hat{g}(\eta;w^*) + \frac{\partial^2\hat{f}(\eta;w^*)}{\partial\eta^2}\right), \tag{29}$$

$$\begin{aligned}N_\theta[\hat{f}(\eta;w^*), \hat{\theta}(\eta;w^*)] = \frac{\partial^2\hat{\theta}(\eta;w^*)}{\partial\eta^2} + \epsilon_1\frac{\partial\hat{\theta}(\eta;w^*)}{\partial\eta}\frac{\partial^2\hat{\theta}(\eta;w^*)}{\partial\eta^2} + \epsilon_1\left(\frac{\partial\hat{\theta}(\eta;w^*)}{\partial\eta}\right)^2\\ + \mathrm{Pr}\begin{pmatrix}\hat{f}(\eta, p)\frac{\partial\hat{\theta}(\eta;w^*)}{\partial\eta} + \delta\hat{\theta}(\eta;w^*) - \delta\gamma_1\hat{f}(\eta, p)\frac{\partial\hat{\theta}(\eta;w^*)}{\partial\eta}\\ - \gamma_1\hat{f}(\eta, p)\frac{\partial\hat{f}(\eta;w^*)}{\partial\eta}\frac{\partial\hat{\theta}(\eta;w^*)}{\partial\eta} - \gamma_1(\hat{f}(\eta, p))^2\frac{\partial^2\hat{\theta}(\eta;w^*)}{\partial\eta^2}\end{pmatrix},\end{aligned} \tag{30}$$

$$\begin{aligned}N_\phi[\hat{f}(\eta;w^*), \hat{\phi}(\eta;w^*)] = \frac{\partial^2\hat{\phi}(\eta;w^*)}{\partial\eta^2} + \epsilon_2\frac{\partial\hat{\phi}(\eta;w^*)}{\partial\eta}\frac{\partial^2\hat{\phi}(\eta;w^*)}{\partial\eta^2} + \epsilon_2\left(\frac{\partial\hat{\phi}(\eta;w^*)}{\partial\eta}\right)^2\\ + \mathrm{Sc}\begin{pmatrix}\hat{f}(\eta, p)\frac{\partial\hat{\phi}(\eta;w^*)}{\partial\eta} - \gamma_2\hat{f}(\eta, p)\frac{\partial\hat{f}(\eta;w^*)}{\partial\eta}\frac{\partial\hat{\phi}(\eta;w^*)}{\partial\eta}\\ - \gamma_2(\hat{f}(\eta, p))^2\frac{\partial^2\hat{\phi}(\eta;w^*)}{\partial\eta^2}\end{pmatrix}.,\end{aligned} \tag{31}$$

The embedding factor is exhibited through w^*; however, auxiliary factors are denoted by $\hbar_f$, $\hbar_g$, $\hbar_\theta$, and $\hbar_\phi$.

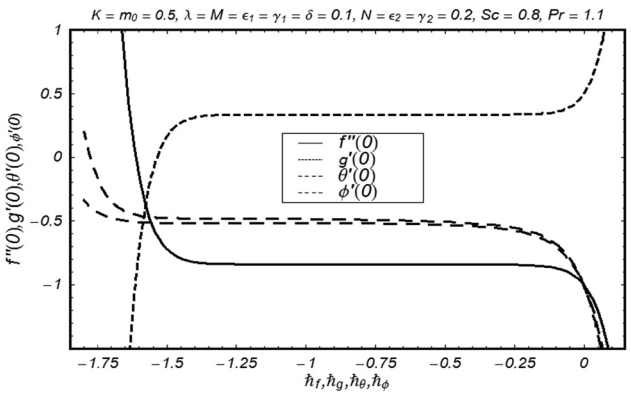

Figure 1: *h*-curve for f, g, θ, and ϕ.

4 Convergence analysis

We used a homotopy scheme [48] to analyze convergent solutions. It is clear that h-curve (s) perform a fundamental part in analyzing the convergence of nonlinear differential systems. That is why the h-curve in Figure 1 is shown to predict our objective. A flat portion of the h-curve helps to obtain usable values of $\hbar_f$ $\hbar_f, \hbar_g, \hbar_\theta$, and $\hbar_\phi$. We examined that $-1.25 \le \hbar_f \le -0.247$, $-1.27 \le \hbar_g \le -0.24$, $-1.5 \le \hbar_\theta \le -0.4$, and $-1.8 \le \hbar_\phi \le -0.4$ along with the assumptions $K = n$ =0.5, $\lambda = 0.1 = M = \epsilon_1 = \delta = \gamma_1$, $N = 0.2 = \epsilon_2 = \gamma_2$, Sc = 0.8, and Pr = 1.1 In addition, converging is seen computationally with the assistance of Table 1. Table 2 displays comparison upshots of employed methodology (HAM) for authentication with earlier simulations of Akbar *et al.* [49]. The analytical upshots of $C_{f_x}\mathrm{Re}_x^{1/2}$ are in decent settlement subjected to different parametric variations of M.

5 Results and discussion

Figures 2–6 reveal the characteristics of distinct variables against the velocity profile $f'(\eta)$. Figure 2 shows that as the vertex velocity K increases, the rapidity outline increases due to the impact of the vertex effect. Figure 3 shows the outcome of the boundary parameter over the velocity

Table 1: Converging investigation in diverse order approximations when $K = n = 0.5$, $\lambda = 0.1 = M = \epsilon_1 = \delta = \gamma_1$, $N = 0.2 = \epsilon_2 = \gamma_2$, Sc = 0.8 and Pr = 1.1

Approximation order	$-f''(0)$	$-g''(0)$	$-\theta'(0)$	$-\phi'(0)$
1	0.8560	0.3780	0.7351	0.7045
5	0.8423	0.3750	0.5576	0.5374
10	0.8402	0.3742	0.5263	0.5018
15	0.8394	0.3739	0.5183	0.4895
20	0.8390	0.3738	0.5161	0.4836
30	0.8388	0.3737	0.5159	0.4825
40	0.8388	0.3737	0.5159	0.4825

Table 2: Comparative outcomes featuring $C_{fx}\mathrm{Re}_x^{\frac{1}{2}}$ for different estimations of M.

M	Ref. [49]	Present findings
0.0	−1.00000	−1.00000
0.3	−1.01980	−1.01980
0.5	−1.11803	−1.11803
0.7	−1.28063	−1.28062
1.0	−1.41421	−1.41421

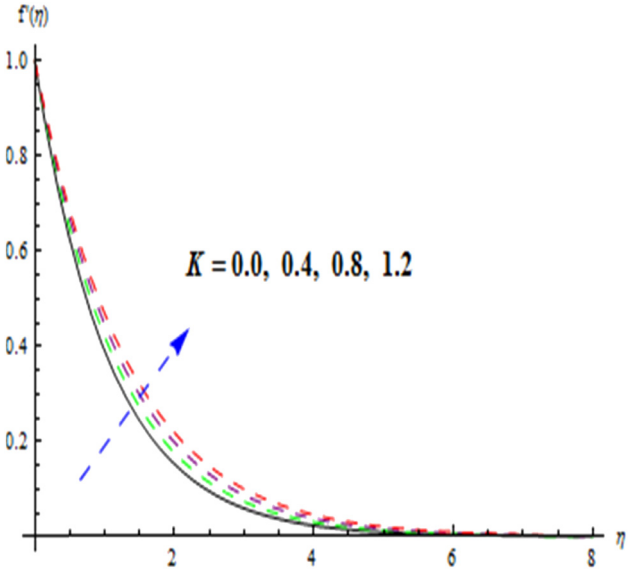

Figure 2: Influences of vertex velocity K on flow $f'(\eta)$.

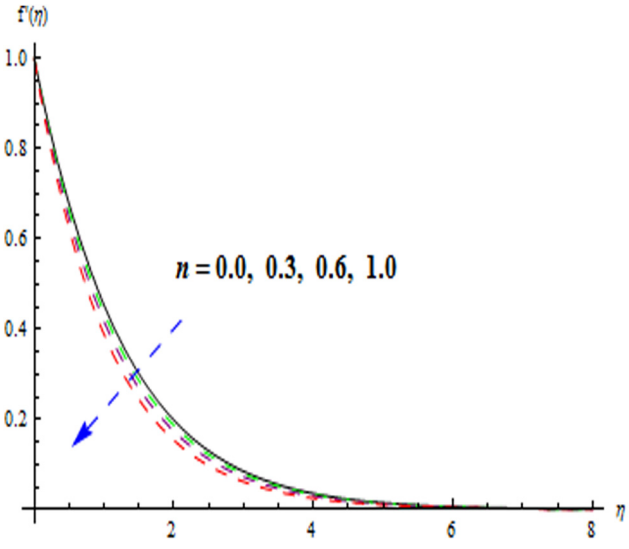

Figure 3: Influences of boundary parameter n on flow $f'(\eta)$.

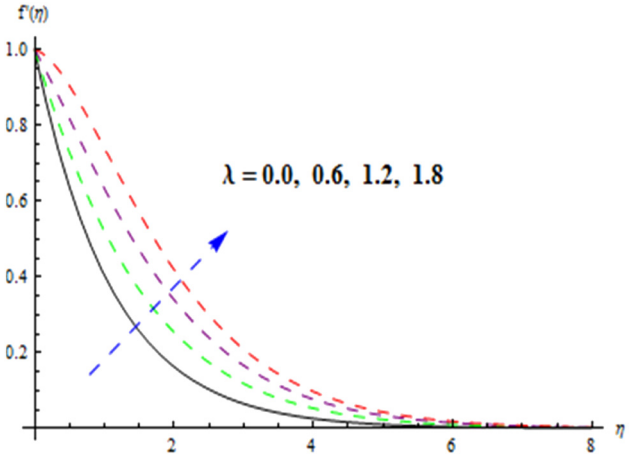

Figure 4: Influences of relaxation time flux λ on flow $f^{'}(\eta)$.

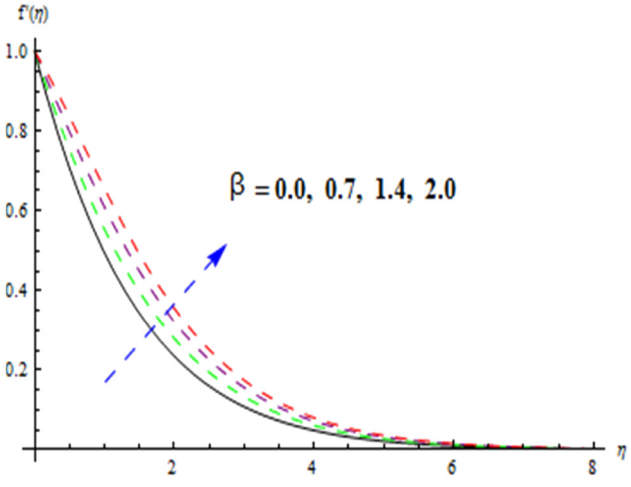

Figure 5: Influences of expansion coefficient β on flow $f^{'}(\eta)$.

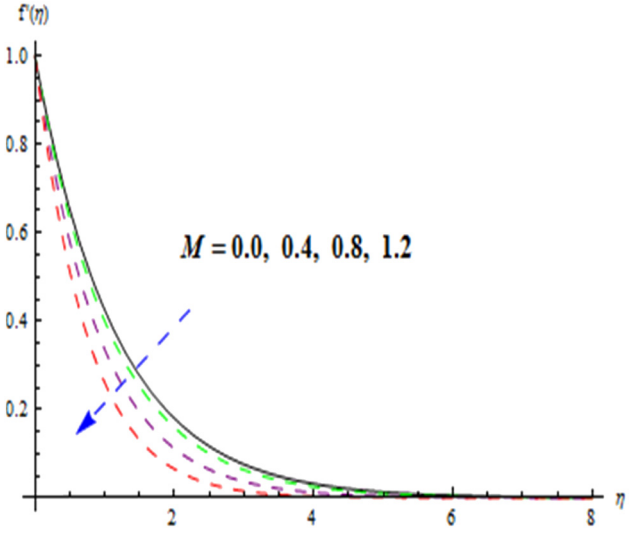

Figure 6: Influences of magnetic field M on flow $f^{'}(\eta)$.

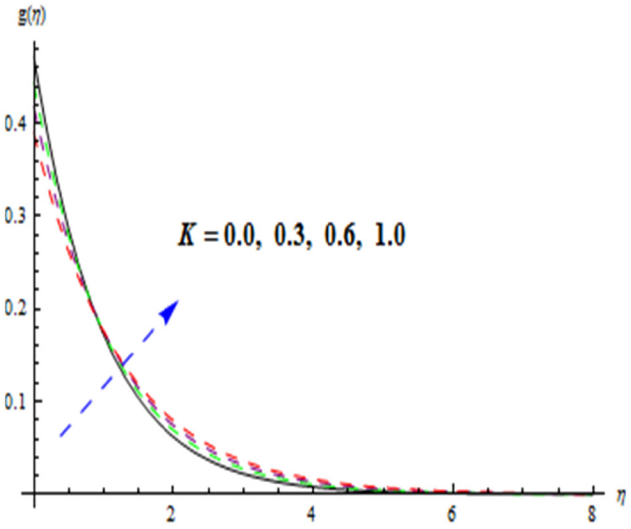

Figure 7: Influences of vertex velocity K on flow $g(\eta)$.

profile, which shows that the velocity function declines due to a mass of the value of boundary parameter n. Figure 4 interprets the difference in the rapidity function for diverse amounts of λ. It shows that relaxation time flux λ increases the velocity due to improved momentum. Figure 5 depicts the micro-rotation velocity against the velocity profile. It illustrates assistance gained by the flow velocity from the micro-rotational aspects. Figure 6 clearly expresses the impact of the Lorentz force due to increasing magnetic field M which suppresses the flow velocity. Figures 7 and 8 show that lateral directional flow $g(\eta)$ increases for larger values of vertex velocity K and vortex rotation N.

Figure 9 reports arbitrary thermal conductivity ϵ_1 characteristics on $\theta(\eta)$. Clearly, $\theta(\eta)$ increases as ϵ_1 increases due to increased thermal conductivity, which assists the heat

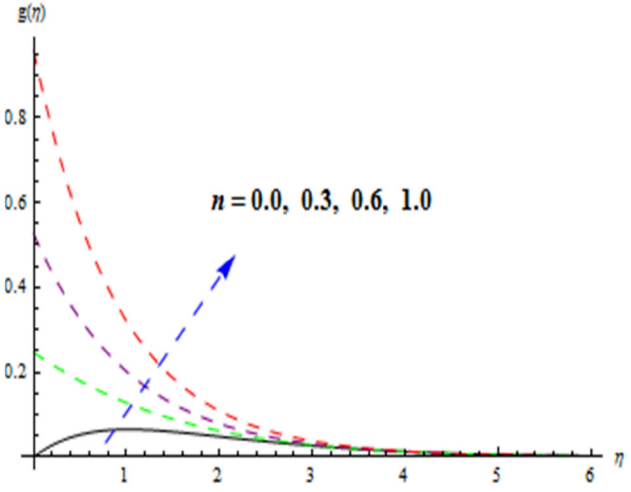

Figure 8: Influences of boundary parameter n on flow $g(\eta)$.

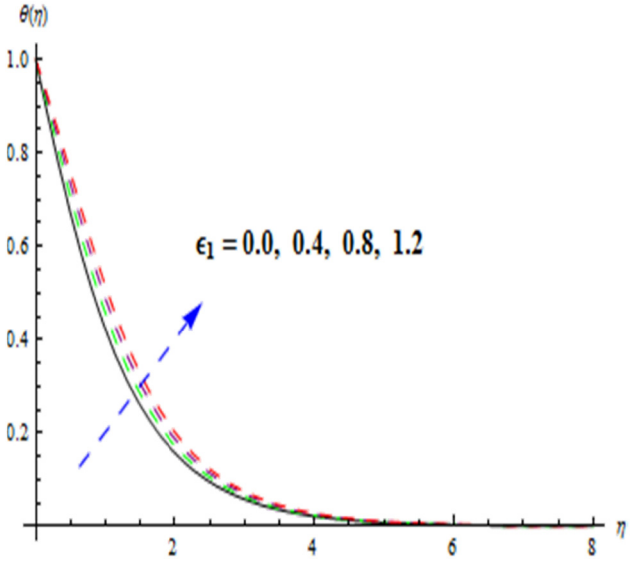

Figure 9: Influences of arbitrary thermal conductivity ϵ_1 on thermal dispersal $\theta(\eta)$.

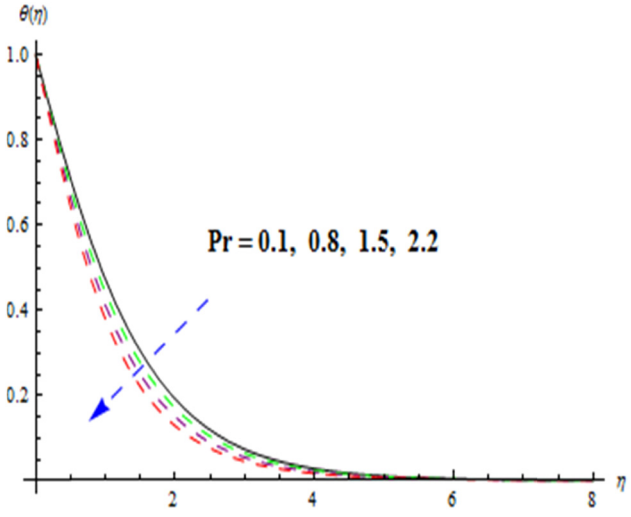

Figure 10: Effects of Prandtl number Pr on thermal dispersal $\theta(\eta)$.

transfer. Figure 10 elaborates that a larger Pr value yields less diffusivity which reduces the temperature profile $\theta(\eta)$. Figure 11 addresses ($\delta > 0$) the heat generation and ($\delta < 0$) heat absorption variables against the temperature profile $\theta(\eta)$. It illustrates that $\delta > 0$ increases the temperature dispersal due to improved heat generation, whereas $\delta < 0$ decreases the temperature dispersion $\theta(\eta)$ due to heat absorption. Figure 12 depicts that the temperature profile decreases by increasing the values of the velocity spin gradient γ_1, which is related to the non-conductivity comportment caused by which $\theta(\eta)$ decreases. Figure 13 shows the behavior of the thermal spin gradient γ_2.

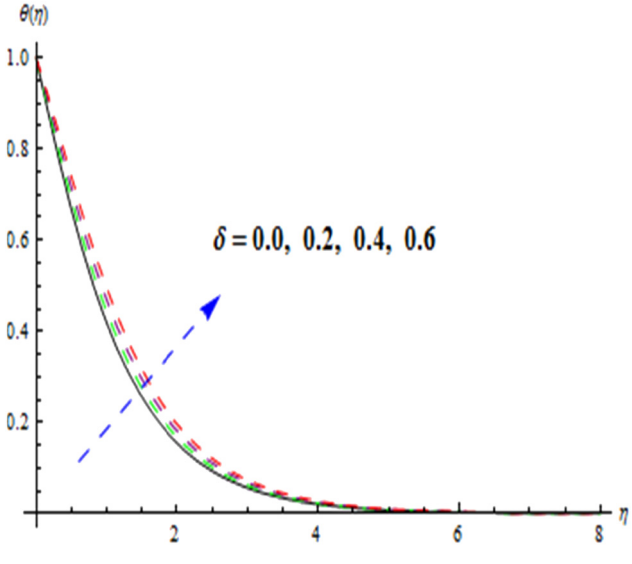

Figure 11: Effects of Heat generation δ on thermal dispersal $\theta(\eta)$.

Figure 14 shows the Schmidt number Sc and its impact on concentration dispersal $\phi(\eta)$. Here, flow concentration $\phi(\eta)$ reduces by increasing Sc values work against the mass transference process. Schmidt number Sc describes Brownian diffusivity which has opposite behavior with concentration dispersal. Figure 15 shows the characteristics of arbitrary mass diffusivity ϵ_2 on flow concentration $\phi(\eta)$. It is clear that larger values of ϵ_2 improves mass diffusivity, which raises the flow concentration $\phi(\eta)$. Figures 16 and 17 illustrate the influence of vertex velocity K and relaxation time flux λ the skin friction, respectively. Vertex velocity K favors the flow movement, which acts against skin friction, while relaxation time flux λ enhances the skin friction due to more contact time availability between fluid and the surface.

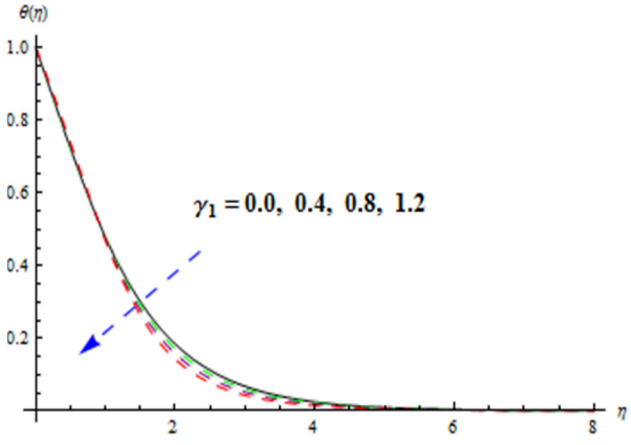

Figure 12: Effects of spin gradient viscosity γ_1 on thermal dispersal $\theta(\eta)$.

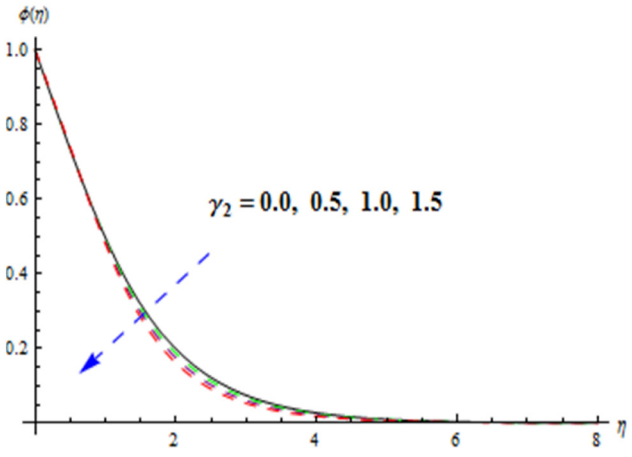

Figure 13: Effects of spin gradient viscosity γ_2 on thermal dispersal $\theta(\eta)$.

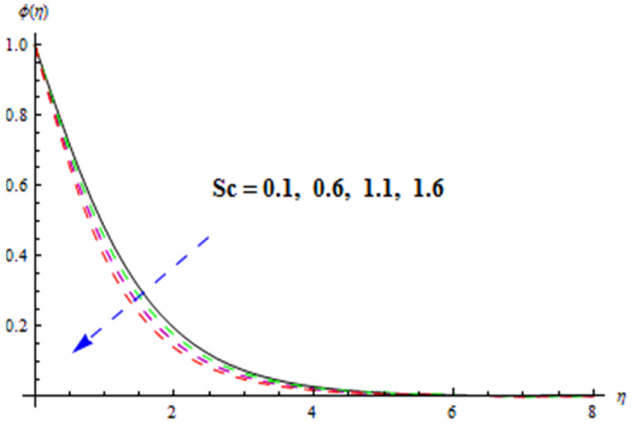

Figure 14: Effects of Schmidt number Sc on concentration $\phi(\eta)$.

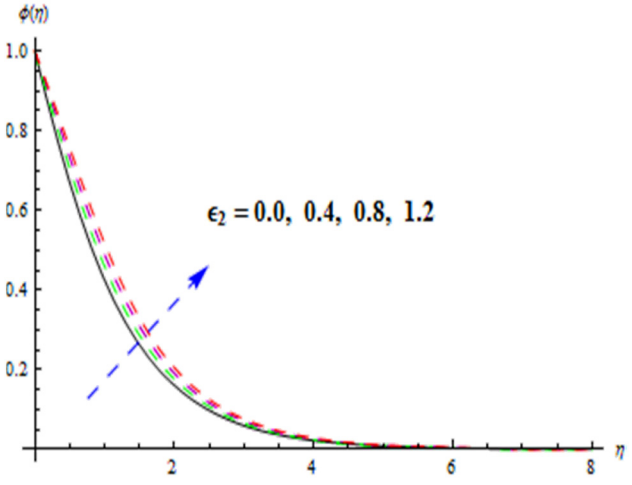

Figure 15: Effects of arbitrary concentration parameter ϵ_2 on concentration $\phi(\eta)$.

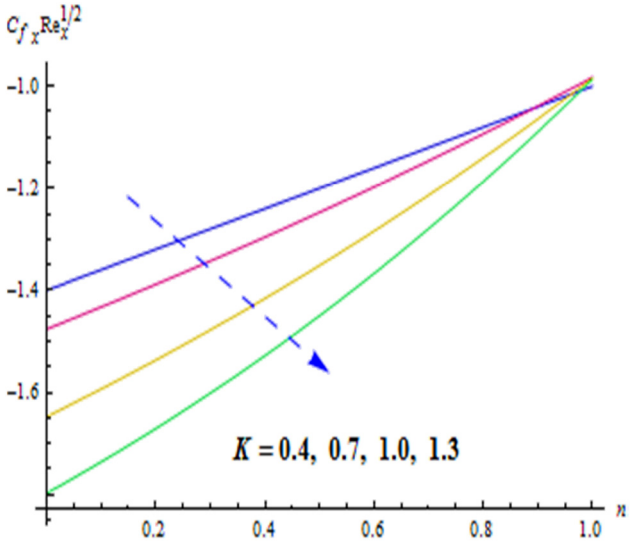

Figure 16: Effects of vertex velocity K on Skin friction $C_{f_x}\mathrm{Re}_x^{1/2}$.

6 Final remarks

In the occurrence of the generalized Fourier–Fick rule, we examined how the temperature-dependent features of the micropolar fluids affected the flow of the MHD fluids as they passed through the vertical linear stretchable sheet. In order to get the numerical findings, an effective version of the HAM was used. The following is a list of the major results obtained from this work:

- For higher micro-planar rotation, the velocity and micropolar functions get elevated.

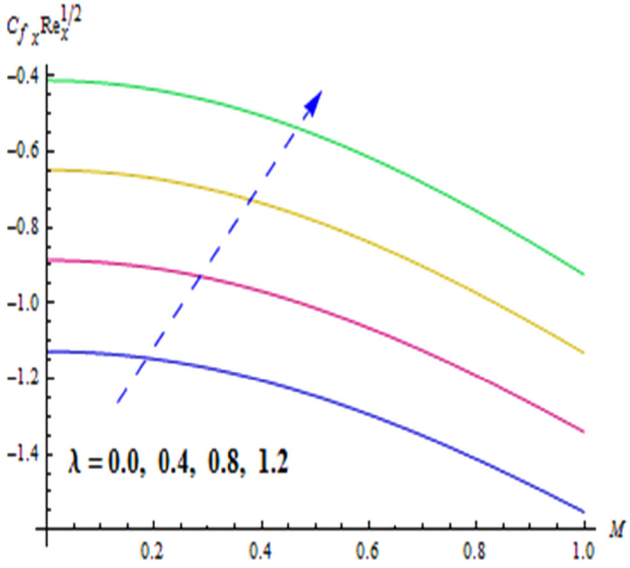

Figure 17: Effects of relaxation time flux λ on Skin friction $C_{f_x}\mathrm{Re}_x^{1/2}$.

- Constraints like solutal and thermal expansions work in favor of the flow to increase its velocity while the magnetic field parameter tends to suppress the flow through the Lorentz force.
- Thermal dispersal gets assisted by thermal conductivity ϵ_1 and both cases of $\delta > 0$ and $\delta < 0$ heat generation constraints are for higher values of ϵ_1 and temperature profile declines due to higher values of Prandtl number Pr and Spin gradient γ_1.
- Concentration dispersal $\phi(\eta)$ gets improved for the increasing diffusivity ϵ_2, on contrary the Spin gradient γ_2 and Schmidt number Sc.
- The skin friction decreases for the viscous alterations K and time relaxation constraints λ.

7 Future insights

In this work, the effects of MHD-based micropolar fluid flow with temperature-dependent properties on a vertical stretching sheet under Fourier–Fick laws were studied. It could create a greater impact on the thermal and mass transfer research stream. In the future, such concepts can be extended for flow past various geometries with numerous types of fluids such as nanofluid, hybrid nanofluid, and ferrofluids. The existing scheme could be applied to a variety of physical and technical challenges in the future.

Funding information: The authors state no funding involved.

Author contributions: Conceptualization: Muhammad Imran Anwar; formal analysis: Muhammad Saqlain; investigation: Muhammad Waqas, M. Prakash, and Abdul Wahab; Methodology: Muhammad Waqas, M. Prakash, and Abdul Wahab; software: Wasim Jamshed; writing – original draft: Mohamed R. Eid; validation: Wasim Jamshed and Mohamed R. Eid; re-graphical representation: Nek Muhammad Katbar; computational process breakdown: Yijie Li; Re-modelling design: Ahmed M. Hassan. All authors have accepted responsibility for the entire content of this manuscript and approved its submission.

Conflict of interest: The authors state no conflict of interest.

Data availability statement: All data generated or analyzed during this study are included in this published article.

References

[1] Fourier JB. Théorie analytique de la chaleur. F. Didot, Cambridge; 1822.
[2] Cattaneo C. A form of heat conduction equation which eliminates the paradox of instantaneous propagation. Comput Rend Math. 1958;247:431–3.
[3] Christov CI. On frame indifferent formulation of the Maxwell-Cattaneo model of finite speed heat conduction. Mech Res Commun. 2009;36:481–6.
[4] Zubair M, Waqas M, Hayat T, Ayub M, Alsaedi A. The onset of modified Fourier and Fick's theories in temperature dependent conductivity flow of micropolar liquid. Res Phys. 2017;7:3145–52.
[5] Waqas M, Hayat T, Shehzad SA, Alsaedi A. Application of improved Fourier's and Fick's laws in a non-Newtonian fluid with temperature-dependent thermal conductivity. J Braz Soc Mech Sci Eng. 2018;40:116.
[6] Sui J, Zhao P, Cheng Z, Zheng L, Zhang X. A novel investigation of a micropolar fluid characterized by nonlinear constitutive diffusion model in boundary layer flow and heat transfer. Phys Fluids. 2017;29:023105.
[7] Waqas M, Khan MI, Hayat T, Alsaedi A. Generalized Fourier and Fick's perspective for stretching flow of Burgers fluid with temperature-dependent thermal conductivity. Therm Sci. 2019;24:3425–32.
[8] Anwar MI, Saqlain M, Gulzar MM, Waqas M. A modified Fourier-Fick analysis for modelling non-Newtonian mixed convective flow considering heat generation. Therm Sci. 2020;23:1381–7.
[9] Khan M, Hussain A, Malik MY, Salahuddin T, Aly S. Numerical analysis of Carreau fluid flow for generalized Fourier's and Fick's laws. Appl Numer Math. 2019;144:100–17.
[10] Khan M, Ahmad L, Khan WA, Al ASZ. Shamrani, The application of non-Fourier and Fick's laws to the flow of temperature-dependent thermal conductivity generalized Newtonian liquids: A 3D computational study. Sci Iran C. 2019;26(3):1516–28.
[11] Hayat T, Javed M, Imtiaz M, Alsaedi A. Effect of Cattaneo-Christov heat flux on Jeffrey fluid flow with variable thermal conductivity. Res Phys. 2018;8:341–51.
[12] Devi SPA, Prakash M. Temperature dependent viscosity and thermal conductivity effects on hydromagnetic flow over a slandering stretching sheet. J Nigerian Math Soc. 2015;34:318–30.
[13] Han S, Zhang L, Li C, Zhang X. Coupled flow and heat transfer in viscoelastic fluid with Cattaneo-Christov heat flux model. Appl Math Lett. 2014;38:87–93.
[14] Muhammad N, Nadeem S, Mustafa T. Squeezed flow of a nanofluid with Cattaneo-Christov heat and mass fluxes. Results Phys. 2017;7:862–9.
[15] Mahanthesh B, Gireesha BJ, Raju CSK. Cattaneo-Christov heat flux on UCM nanofluid flow across a melting surface with double stratification and exponential space dependent internal. Info Med Unlocked. 2017;9:26–34.
[16] Daneshjou K, Bakhtiari M, Parsania H, Fakoor M. Non-Fourier heat conduction analysis of infinite 2D orthotropic FG hollow cylinders subjected to time-dependent heat source. Appl Therm Eng. 2016;98:582–90.
[17] Khan WA, Irfan M, Khan M, Alshomrani AS, Alzahrani AK, Alghamdi MS. Impact of chemical processes on magneto nanoparticle for the generalized Burgers fluid. J Mol Liq. 2017;234:201–8.
[18] Fourier JBJ. Analytique Théorie De La Chaleur. F. Didot, Paris; 1822.

[19] Alsaedi A, Alsaadi FE, Ali S, Hayat T. Stagnation point flow of Burgers' fluid and mass transfer with chemical reaction and porosity. J Mech. 2013;29:453–60.
[20] Tibullo V, Zampoli V. A uniqueness result for the Cattaneo-Christov heat conduction model applied to incompressible fluids. Mech Res Commun. 2011;38:77–9.
[21] Waqas M, Hayat T, Shehzad SA, Alsaedi A. Analysis of forced convective modified Burger's liquid flow considering Cattaneo-Christov double diffusion. Results Phys. 2018;8:908–13.
[22] Khan M, Salahuddin T, Malik MY. An immediate change in viscosity of Carreau nanofluid due to double stratified medium: application of Fourier's and Fick's laws. J Braz Soc Mech Sci Eng. 2018;40:457.
[23] Waqas M, Shehzad SA, Hayat T, Khan MI, Alsaedi A. Simulation of magnetohydrodynamics and radiative heat transport in convectively heated stratified flow of Jeffrey nanofluid. J Phys Chem Solids. 2019;133:45–51.
[24] Eringen AC. Theory of micro-polar fluids. J Math Mech. 1966;16:1–18.
[25] Khedr MEM, Chamkha AJ, Bayomi M, Flow MHD. of a micro-polar fluid past a stretched permeable surface with heat generation/absorption. Nonlinear Anal Model Control. 2009;14:27–40.
[26] Ishak A. Thermal boundary layer flow over a stretching sheet in a micropolar fluid with radiation effect. Meccanica. 2010;45:367–73.
[27] Hussain M, Ashraf M, Nadeem S, Khan M. Radiation effects on the thermal boundary layer flow of a micropolar fluid towards a permeable stretching sheet. J Franklin Inst. 2013;350:194–210.
[28] Aurangzaib M, Uddin S, Bhattacharyya K, Shafie S. Micropolar fluid flow and heat transfer over an exponentially permeable shrinking sheet. Propul Power Res. 2016;5:310–7.
[29] Haque MZ, Alam MM, Ferdows M, Postelnicu A. Micro-polar fluid behaviors on steady MHD free convection and transfer flow with constant heat and mass fluxes, joule heating and viscous dissipation. J King Saud Univ Eng Sci. 2012;24:71–84.
[30] Subhani M, Nadeem S. Numerical investigation into unsteady magnetohydrodynamics flow of micropolar hybrid nanofluid in porous medium. Phys Scr. 2019;94:105220.
[31] Shehzad SA, Abbas Z, Rauf A. Finite difference approach and successive over relaxation (SOR) method for MHD micropolar fluid with Maxwell-Cattaneo law and porous medium. Phys Scr. 2019;94:115228.
[32] Zaib A, Haq RU, Sheikholeslami M, Khan U. Numerical analysis of effective Prandtl model on mixed convection flow of Al_2O_3-H_2O nanoliquids with micropolar liquid driven through wedge. Phys Scr. 2020;95:035005.
[33] Fang T, Zhang J, Zhong YF. Boundary layer flow over a stretching sheet with variable thickness. Appl Math Comput. 2012;218:7241–52.
[34] Khader MM, Megahed AM. Boundary layer flow due to a stretching sheet with a variable thickness and slip velocity. J Appl Mech Tech Phys. 2015;56:241–7.
[35] Hayat T, Khan MI, Farooq M, Alsaedi A, Waqas M, Yasmeen T. Impact of Cattaneo–Christov heat flux model in flow of variable thermal conductivity fluid over a variable thicked surface. Int J Heat Mass Tran. 2016;99:702–10.
[36] Cortell R. Viscous flow and heat transfer over a nonlinearly stretching sheet. Appl Math Comput. 2007;184:864–73.
[37] Yang W, Chen X, Zhang X, Zheng L, Liu F. Flow and heat transfer of double fractional Maxwell fluids over a stretching sheet with variable thickness. Appl Math Model. 2019;10:55–63.
[38] Abdel-wahed MS, Elbashbeshy EMA, Emam TG. Flow and heat transfer over a moving surface with non-linear velocity and variable thickness in a nanofluids in the presence of Brownian motion. Appl Math Comput. 2015;254:49–62.
[39] Ragupathi P, Ahammad NA, Wakif A, Shah NA, Jeon Y. Exploration of multiple transfer phenomena within viscous fluid flows over a curved stretching sheet in the co-existence of gyrotactic microorganisms and tiny particles. Mathematics. 2022;10(21):4133.
[40] Wakif A, Shah NA. Hydrothermal and mass impacts of azimuthal and transverse components of Lorentz forces on reacting Von Kármán nanofluid flows considering zero mass flux and convective heating conditions. Waves Random Complex Media. 2022. doi: 10.1080/17455030.2022.2136413.
[41] Eswaramoorthi S, Loganathan K, Faisal M, Botmart T, Shah NA. Analytical and numerical investigation of Darcy-Forchheimer flow of a nonlinear radiative non-Newtonian fluid over a Riga plate with entropy optimization. Ain Shams Eng J. 2023;14(3):101887.
[42] Alghamdi W, Alsubie A, Kumam P, Saeed A, Gul T. MHD hybrid nanofluid flow comprising the medication through a blood artery. Sci Rep. 2021;11:11621.
[43] Saeed A, Alghamdi W, Mukhtar S, Shah SI, Kumam P, Gul T, et al. Darcy-Forchheimer hybrid nanofluid flow over a stretching curved surface with heat and mass transfer. PLoS One. 2021;16(5):e0249434.
[44] Gul T, Noman W, Sohail M, Khan MA. Impact of the Marangoni and thermal radiation convection on the graphene-oxide-water-based and ethylene-glycol-based nanofluids. Adv Mech Eng. 2019;11(6):1687814019856773.
[45] Irfan M, Khan WA, Pasha AA, Alam MI, Islam N, Zubair M. Significance of non-Fourier heat flux on ferromagnetic Powell-Eyring fluid subject to cubic autocatalysis kind of chemical reaction. Int Commun Heat Mass Transf. 2022;138:106374.
[46] Anjum N, Khan WA, Hobiny A, Azam M, Waqas M, Irfan M. Numerical analysis for thermal performance of modified Eyring Powell nanofluid flow subject to activation energy and bioconvection dynamic. Case Stud Therm Eng. 2022;39:102427.
[47] Tabrez M, Khan WA. Exploring physical aspects of viscous dissipation and magnetic dipole for ferromagnetic polymer nanofluid flow. Waves Random Complex Media. 2022. doi: 10.1080/17455030.2022.2135794.
[48] Liao S. On the homotopy analysis method for nonlinear problems. Appl Math Comput. 2004;147:499–513.
[49] Akbar NS, Nadeem S, Haq RU, Khan ZH. Numerical solutions of Magnetohydrodynamic boundary layer flow of tangent hyperbolic fluid towards a stretching sheet. Indian J Phys. 2013;87:1121–4.